

Direct conversion of human fibroblasts into therapeutically active vascular wall-typical mesenchymal stem cells

Jennifer Steens¹, Kristian Unger², Anika Neureiter³, Karolin Wieber¹, Julia Hess², Heinz G. Jakob⁴, Hannes Klump³, Diana Klein¹

¹Institute for Cell Biology (Cancer Research), University Hospital Essen, University of Duisburg-Essen, Essen, Germany

²Research Unit Radiation Cytogenetics, Helmholtz Zentrum München, German Research Center for Environmental Health GmbH, Neuherberg, Germany

³Institute for Transfusion Medicine, University Hospital Essen, University of Duisburg-Essen, Essen, Germany

⁴Department of Thoracic and Cardiovascular Surgery, West-German Heart and Vascular Center Essen, University Duisburg-Essen, Germany

Correspondence to

PD Dr. Diana Klein

Institute of Cell Biology (Cancer Research)

Medical Faculty, University of Duisburg-Essen

Virchowstr. 173, Ger-45122 Essen

Tel:+49-201-723 83342

Fax:+49-201-723 5904

E-mail: Diana.Klein@uk-essen.de or Hannes.Klump@uk-essen.de

Running Title

VW-MSCs directly converted from fibroblasts

Summary

Cell-based therapies using adult stem cells are a promising option for the treatment of a number of diseases including autoimmune and cardiovascular disorders. Among these, vascular wall-derived mesenchymal stem cells (VW-MSCs) are particularly well suited for the protection and curative treatment of vascular damage because of their tissue-specific action. Here we report on the direct conversion of human skin fibroblasts towards MSCs using a VW-MSC-specific gene code (HOXB7, HOXC6 and HOXC8) thereby avoiding the detour via reprogramming towards iPSCs and subsequent directed differentiation. This direct programming approach successfully mediated the generation of VW-typical MSCs with classical MSC characteristics *in vitro* and *in vivo*. With respect to their therapeutic potential, these cells suppressed lymphocyte proliferation, and protected mice against vascular damage in a mouse model of radiation-induced pneumopathy. The feasibility to obtain patient-specific, VW-MSCs from fibroblasts in large amounts by forward programming could potentially open avenues towards novel, MSC-based therapies.

Keywords

Vascular wall, mesenchymal stem cells, *HOX* gene, fibroblast, direct conversion, stem cell therapy

Introduction

Tissue stem cells offer a promising therapeutically option for the prevention and treatment of a number of diseases, such as neurological, autoimmune and cardiovascular disorders, and various cancers e.g., leukemia¹⁻⁵. So-called multipotent mesenchymal stem cells (MSCs), also called mesenchymal stromal cells, have been described to home to particular anatomical sites after transplantation and differentiate into specific cell types to locally replace the damaged tissue. Thus, they are especially interesting for use in cell replacement therapies. In addition, MSCs have been genetically modified to enable targeted delivery of a variety of therapeutic agents in malignant diseases^{4,6,7}. Today it is widely accepted that MSCs can preserve existing functional tissue from further destruction or support regenerative processes by paracrine mechanisms such as the synthesis and secretion of protective growth factors and cytokines⁸⁻¹⁰. It has been suggested that MSCs mediate their function through a 'hit and run' mechanism, during which MSCs transiently provide a local source of trophic factors in the local environment during temporary localization to the targeted tissue^{8,11,12}. Thus, therapeutically applied MSCs could be able to rescue injured tissue by reducing damage and accelerating its repair. Furthermore, MSCs exert immune-regulatory activities as they can suppress the T cell response^{13,14}. The immunosuppressive effects of MSCs make them attractive candidates for a variety of cellular therapies, including treatment of immune disorders. These unique properties have promoted wide application of MSCs in clinical trials to treat a wide range of diseases caused by dysregulation of the adaptive immune system (www.clinicaltrials.gov). Transplantation of bone marrow-derived MSCs has established itself as a possible strategy for the treatment of graft versus host disease, chronic obstructive pulmonary disease, Crohn's disease or even multiple sclerosis¹⁵⁻¹⁷. During ontogenesis, MSCs originate from the mesenchyme and are involved in the development of all tissues and organs which develop from the mesenchyme. In the adult organism, embryonic mesenchyme is absent, but almost all tissues harbor reservoirs of MSCs that contribute to the maintenance of organ integrity by replacing lost cells or by locally secreting cytokines, thereby supporting repair and healing of tissues^{18,19}. Although bone marrow is the most frequently used source for obtaining MSCs, they can also be obtained from umbilical cord blood, placenta, blood, fetal liver, adipose tissue and, also from the wall of adult blood vessels²⁰⁻²⁴. However, the proportion of MSCs contained in primary isolates is rather low. Therefore, alternative, more accessible sources for MSCs are needed.

An alternative method for obtaining MSCs is by directed differentiation of embryonic stem (ES-) or induced pluripotent stem cells (iPSCs), *in vitro*, which allows for the generation of MSCs in large quantities and with comparable properties²⁵⁻²⁸. iPSCs present an unlimited source for a broad range of applications including disease modeling, drug development, toxicity testing, *in vitro*, as well as cell-replacement therapies, *in vivo*²⁹⁻³¹. Several studies have reported the successful generation of MSCs from human iPSCs³²⁻³⁴. However, their clinical use has been hampered by the tumorigenic potential elicited by undifferentiated iPSCs potentially remaining in the differentiated cell population, the lengthy and inefficient differentiation process, and genomic instability due to suboptimal culture conditions. A possible solution to these drawbacks could be to directly program an easily accessible somatic cell type such as fibroblasts towards MSCs.

We recently reported the *in vitro* generation of vascular wall (VW)-typical MSCs from mouse iPSCs, based on a vascular wall MSCs specific gene code^{35,36}. Herein, a lentiviral vector expressing a small set of human vascular wall MSCs-specific HOX-genes (*HOXB7*, *HOXC6* and *HOXC8*) was used to directly program iPSCs into VW-MSCs which displayed classical MSC characteristics, both *in vitro* and *in vivo*³⁵. In this work, we asked whether ectopic expression of the same HOX-genes could be used for directly converting somatic cells towards MSCs, thereby avoiding the detour via iPSCs. We show that human skin fibroblasts can be directly converted

towards vascular wall-typical multipotent stem cells of mesenchymal nature by ectopic lentiviral expression of our previously defined VW-MSc specific *HOX*-code encompassing *HOXB7*, *HOXC6* and *HOXC8*.

Results

Generation of VW-typical MSCs by direct lineage conversion

To test whether vascular wall-specific MSCs can specifically be obtained by direct conversion of primary human fibroblasts *in vitro*, primary fibroblasts of different healthy donors were transduced with a self-inactivating (SIN) lentiviral vector co-expressing the coding sequences of *HOXB7*, *HOXC6* and *HOXC8* separated by 2A esterase elements, together with the gene encoding mTurquoise2 (mCyan-derived) fluorescent protein³⁵ (Fig. 1a). Transduced fibroblasts were sorted for mTurquoise2-fluorescence 2-4 days after transduction and further cultivated (Fig. 1b). The process of transduction resulted in a more flattened MSC-typical phenotype as compared to the elongated cell morphology of control transduced fibroblasts (Fig. 1b). Expression of the endogenous and ectopic HOX proteins was confirmed by Western blot (Fig. 1d) and immunocytochemistry (Fig. 1e). As expected, increased cytoplasmic as well as a prominent nuclear localization of the HOX proteins were observed in HOX-transduced fibroblasts. Steady-state endogenous and vector-mediated *HOX* transcription was further quantified by qRT-PCR (Fig. 2a and Supplementary Fig. 1). Significantly increased ectopic *HOXB7*, *HOXC6* and *HOXC8* mRNA expression levels were only detected in HOX-transduced fibroblasts. Of note, the classical MSC marker (CD90, CD73, CD105) gene expressions as well as respective protein expressions were expressed in fibroblasts at similar levels (Fig. 2a and Supplementary Fig. 1 and 2), which resulted only in a further increase of the MSC marker expression levels by tendency. Cell proliferation was not affected by transduction as HOX- as well as control transduced and FACS-purified fibroblasts showed similar proliferative activities (Supplementary Fig. 2).

To test for the propensity of the fibroblast-derived, induced MSCs to differentiate towards adipocytes, osteoblasts and chondrocytes, the cells were plated and cultured in appropriate differentiation media for additional 14 days (Fig. 2b and Supplementary Fig. 3). Adipogenic, osteogenic as well as chondrogenic differentiation of fibroblast-derived MSCs was more efficient when the three *HOX* genes were ectopically expressed as confirmed by the quantification of the significantly increased expression levels of the differentiation marker genes peroxisome proliferator-activated receptor gamma (adipocytes), alkaline phosphatase and osteocalcin (osteocytes) and aggrecan (chondrocytes) upon differentiation (Fig. 2c). To test whether the HOX-induced, putative VW-MSCs are able to contribute to the morphogenesis of functional blood vessels, *in vivo*, we subcutaneously co-transplanted the transduced cells together with endothelial cells in Matrigel into immune-deficient NMRI nude mice (Fig. 2d and Supplementary Fig. 4). After 14 days Matrigel plugs were re-isolated and human CD31 and Turquoise 2 reporter-fluorescence was detected. Formation of new blood vessels within the plugs was demonstrated by the presence of vessels lined by CD31-positive endothelial cells. Turquoise2/HOX-positive cells were closely associated to these vessels displaying a flattened and elongated phenotype, thus indicating the potential differentiation of induced and co-implanted VW-MSCs towards vascular mural cells, e.g. pericytes and smooth muscle cells. Compared to plugs containing control-transduced fibroblasts, plugs with fibroblast-derived VW-

MSCs showed a stronger vascularization and larger, more stabilized newly formed blood vessels (Fig. 2d and Supplementary Fig. 4). Fibroblast-derived MSC-differentiation into pericytes was further confirmed by co-immunostaining of the pericytes/smooth muscle cell marker smooth muscle actin (ACTA2) and the reporter protein Turquoise 2/CFP (Supplementary Fig. 4). In addition, the propensity for CFU (colony forming unit)-formation was significantly higher in induced MSCs derived from HOX-transduced fibroblasts as compared to the controls (Fig. 2e and Supplementary Fig. 2). To test whether the HOX-transduced cells became tumorigenic, NMRI nude mice were subcutaneously injected with HOX- as well as control-transduced cells. No tumor growth was observed for all implanted cell charges following 60 days after tumor implantation (0/8 per HOX/Ctrl transduction each; transduced fibroblasts from two independent donors were investigated) (not shown).

Comparative global profiling of generated VW-MSCs

To investigate to which extent human fibroblast-derived VW-MSCs resemble ex vivo isolated human internal thoracic artery (hITA)-derived VW-MSCs, we compared the global gene expression and DNA methylation (DNAm) profiles of the generated VW-MSCs to those of control-transduced fibroblasts and hITA-derived VW-MSCs (Fig. 3). Global gene expression analysis showed that the gene expression profiles of ectopic *HOX*-expressing fibroblasts clustered together and were closely related to hITA-derived VW-MSC but distinct from control-transduced fibroblasts (Fig. 3a,b). The principle component analysis using the Rohart MSC signature genes³⁷ extracted from the global gene expression profiles of the confirmed that close relationship (Fig. 3b). To assess whether the obtained global transcriptome profiles display a signature similar to primary MSCs, we performed Gene Set Enrichment Analysis (GSEA)³⁸ using gene sets from the Molecular Signatures Database (MSigDBv.3.0) (Supplementary Fig. 5). We found 46 gene sets shared with VW-MSC (for complete list see Supplementary Table 1), of which 23 gene sets were also found in the induced fibroblast-derived MSCs clearly indicating that HOX-transduced fibroblasts were more closely related to VW-MSCs isolated from human vessels than to control transduced fibroblasts (Fig. 3a, b and Supplementary Fig. 5). Analysis of the DNAm profiles of the different cell preparations revealed that generated VW-MSCs were more closely to the hITA-derived VW-MSCs while control-transduced fibroblasts cluster together with the donor material (primary fibroblasts) (Fig. 3c, d).

In summary, the ectopic expression of three MSC-specific HOX genes promoted the in vitro differentiation of fibroblasts towards vascular wall-typical and thus HOX-positive multipotent MSCs.

The transcriptional signature of induced fibroblast-derived VW-MSCs ectopically expressing HOXB7, HOXC6 and HOXC8 confirms the acquisition of a MSC phenotype

To further confirm if the induced VW-MSCs displayed a gene expression signature corresponding to classical and well-known MSCs we again performed GSEA (Fig. 4 and Supplementary Table 2). We first used the gene sets specific for MSCs derived from human placental tissue (PL-MSCs) as compared to primary skin fibroblasts as previously described³⁹. This GSEA uncovered that the induced-VW-MSCs with ectopic expression of the HOX-code most closely resembled a transcriptional signature of PL-MSCs while the control transduced fibroblasts exhibited the typical signature of (skin) fibroblasts (Fig. 4a and Supplementary Table 2). To further refine the analysis we asked how closely these induced VW-MSCs resembled

classical MSCs derived from the bone marrow (BM-MSCs). Again, GSEA indicated a closer relationship of induced fibroblast-derived VW-MSCs to BM-MSCs than control transduced fibroblasts (Fig. 4b-c, and Supplementary Table 2). We finally asked whether the transcriptome of induced VW-MSCs rather displayed the already identified VW-MSC HOX signature using gene sets from VW-MSCs either control or transfected with HOX siRNA³⁶. Again, here GSEA clearly indicated similarity between induced VW-MSC and ex vivo isolated human VW-MSCs (Fig. 4d and Supplementary Table 2). With respect to the suggested therapeutic potential of generated fibroblast-derived VW-MSCs, we compared the transcriptional signature of generated cells to gene sets which were derived from the comparison of ex vivo isolated VW-MSCs to mature human aortic smooth muscle cells (hAoSMC; unpublished gene set). Herein, genes sets were used which comprise genes related to an immunomodulatory function as well as genes involved in angiogenesis (Fig. 4e and Supplementary Table 2). Of note, the induced VW-MSC were highly similar with the ex vivo isolated human VW-MSCs, further supporting our notion that these cells were (i) characterized by a MSC transcriptional phenotype similar to that of VW-MSCs and suggesting that (ii) these cells could be used for therapeutic approach in a preclinical animal model.

Therapeutic potential of generated fibroblast-derived VW-MSCs

To investigate the potential of HOX-induced MSCs to mediate immunomodulation, we next tested their ability to inhibit lymphocyte proliferation using, an allogeneic mixed lymphocyte reaction with different human non-adherent lymphoma cells as mitogens (MOLT17, DoHH2, Jurkat, and U937). Cell-cycle-arrested, irradiated (10 Gy) HOX- and control-transduced cells, as well as VW-MSCs as a positive control, were also used to determine background proliferation during the measurements. Lymphocyte proliferation was determined after 24 hours of co-culture. VW-MSCs, as well as induced MSCs significantly suppressed the proliferation of the different lymphoma cells (Fig. 5a). Thus, we investigated whether therapeutically applied generated VW-MSCs were able to reduce radiation-induced lung fibrosis and endothelial cell loss in a whole thorax irradiation (WTI) model of radiation induced lung disease, established by our group^{40,41} (Fig. 5b and Supplementary Fig. 6). For this, single cell suspensions of cultured induced fibroblast-derived VW-MSC as well as the control cells were intravenously transplanted into the tail vein of irradiated (15 Gy WTI) or untreated C57BL/6 mice, 24 hours after irradiation. Peripheral blood cell analysis within the inflammatory phase at 3 weeks after irradiation revealed decreased total leukocyte numbers upon radiation, whereas treatment with generated fibroblast-derived MSCs normalized these levels by tendency. Of note, a radiation-induced increase of monocyte and granulocyte numbers was normalized in treated animals (Supplementary Fig. 6). Analysis of Turquoise2/HOX expression in isolated lung sections revealed that that nearly none of the therapeutically applied cyan-positive cell homed to the injured lung tissue (not shown). However, circulating induced VW-MSCs could still be detected in peripheral blood several weeks after transplantation (Supplementary Fig. 6). We then analyzed the impact of implanted cells on fibrosis and endothelial cell loss (Fig. 5c,d). Development of radiation-induced fibrosis was investigated 25 weeks after WTI on sections of paraffin-embedded lung tissue and staining by Masson's Goldner Trichrome (connective tissue), and revealed that the therapeutically applied VW-MSCs significantly limited fibrosis development. Treatment with generated fibroblast-derived MSCs significantly also attenuated the synthesis of the pro-fibrotic cytokine TGF- β 1, as detected in homogenized whole lung tissue by Western blot analysis (Fig. 5d). Interestingly, radiation-induced endothelial cell loss was significantly limited in animals which were treated with the induced VW-MSCs as revealed by restored endothelial VE-Cadherin expression in WTI-lungs 25

weeks post irradiation (Fig. 5d). We have to emphasize that the implanted human MSCs or factors derived thereof may not have been as effective as the endogenous mouse-specific factors in terms of tissue-regeneration and/or –protection within this in vivo xenotransplantation model. To test our findings about the radioprotective and/or tissue-regeneration-fostering and, also, paracrine effects of the generated VW-MSCs, we used ex vivo tissue cultures of human normal lung tissue (Fig. 5e). Fresh lung specimens were dissected and embedded in matrigel prior to irradiation with 15Gy, with or without subsequent culture in normal growth media (NGM) alone or NGM supplemented with conditioned media (CM; ratio 1/1), which were derived from cultured fibroblasts, VW-MSCs and Ctrl- and HOX-transduced fibroblasts (generated VW-MSCs). Western blot analyses of total protein extracts confirmed that radiation fostered a (well-known) downregulation of VE-CAD expression and of the associated junctional protein occludin in cultured lung tissues⁴², whilst treatment with conditioned media derived from generated VW-MSCs and hITA-derived VW-MSCs clearly limited endothelial cell loss. We then confirmed restoration of the radiation induced impairment of endothelial cell signaling pathways activated upon CM treatment. Mitogen-activated protein kinase (MAPK) pathways including extracellular signal-regulated kinases 1 and 2 (ERK1/2) and p38 MAPK were restored upon treatment with VW-MSC derived paracrine signals. In addition, the radiation-induced reduction of the antioxidant enzyme superoxide dismutase 1 (SOD1), a MSC-secreted factor involved in radioprotection, adoptively transferred from MSCs⁴¹, was restored in the tissue cultured which were MSC-CM treated (Fig. 5e). The paracrine-based radioprotective action of induced VW-MSCs on the vascular compartment was further confirmed in cultured endothelial cells upon radiation and subsequent MSC-factor treatment (Fig. 5f). Radiation led to a downregulation of VE-CAD expression in cultured endothelial cells, whilst MSC-derived CM limited the reduction (Fig. 5f). Furthermore, expression levels of the proliferation marker Proliferating-Cell-Nuclear-Antigen (PCNA) were restored in MSC CM-treated endothelial cells^{41,42}. Thus, induced VW-MSCs and MSC-derived factors were able to counteract radiation-induced late adverse effects of vascular damage and endothelial cell loss. The high activity of vascular wall-derived MSCs for radioprotection may be due to their tissue-specific action.

Taken together, our results strongly suggest that ectopic expression of MSC-specific HOX genes promotes the conversion of fibroblasts to therapeutically active, vascular wall-typical, multipotent MSCs.

Discussion

Several studies have reported the direct conversion of fibroblasts into cells of other germ layers, such as neurons, hepatocytes, osteoblasts, and cardiac-like myocytes, through enforced expression of lineage-specific transcription factors⁴³⁻⁴⁸. Application of such induced, fully functional cells for autologous cell replacement therapies or tissue engineering derived possesses huge clinical potential. However, large-scale production of specific lineages for regenerative therapies depends on well-defined, highly reproducible culture allowing for significant cell expansion^{29,43,49}.

Different approaches allowing for direct programming of somatic cells can be distinguished: (i) somatic cells can be reprogrammed into iPSCs, (ii) partial reprogramming: a step-wise de-differentiation manner suggesting that re-programming can be controlled and stopped prior to the acquisition of an embryonic-like signature, (ii) direct lineage conversion using transcription factors defining target cell identity, and (iv) chemical-induced conversion^{50,51}. This could be

achieved by transient, ectopic expression of cell-type specific transcription factors, miRNAs or by using of epigenetic modifiers, as shown for other cell types, such as neurons or hepatocyte-like cells⁵²⁻⁵⁵.

However, based on the lack of MSC specific transcription factors which could act as fate-determinants, the direct conversion of fibroblasts towards MSCs using key transcription factors was not yet reported⁴⁶. Noteworthy, drug-mediated conversion of human primary dermal fibroblasts towards induced MSC-like cells was recently reported. A cocktail containing six chemical inhibitors with or without the addition of growth factors was used to induce a MSC-phenotype in fibroblasts⁴⁶. Here, we directly programmed fibroblasts towards vascular wall-typical MSCs by ectopic expression of a small number of *HOX*-genes *in vitro*, namely *HOXB7*, *HOXC6* and *HOXC8*. Those were selected on a *HOX*-code we had previously defined for VW-MSCs^{35,36}. These cells displayed classical multipotent characteristics, *in vitro*, and selectively associated with vascular structures in matrigel plug assays, *in vivo*, thus likely representing true vascular-wall MSCs. Taken together, the generated fibroblast derived VW-MSCs fulfilled all criteria of MSCs as defined by The International Society for Cellular Therapy⁵⁶. Studying well-known MSC markers and their expression profiles in VW-MSCs as compared to human primary fibroblasts we showed here that expression patterns highly overlapped indicating that there is an urgent need in identifying additional cells type-specific markers. In general, it is well known that fibroblasts share a mesenchymal stem cell phenotype. However, important specific features of MSCs are their colony-forming capacity and differentiation potential⁵⁷⁻⁶⁰. In line with these findings we were able to demonstrate here that the generated VW-MSCs displayed significantly increased clonogenicity, and had the capacity to differentiate into chondrocytes, osteocytes and adipocytes, strongly suggesting a mesenchymal stem cell (MSC)-like behavior. These induced cells represented an important source of pericytes and smooth muscle cells during angiogenesis under physiological and pathological conditions. In previous studies we already showed that classical MSC marker proteins, in particular in VW-MSCs, showed a highly overlapping expression profile with other vascular cells, in particular human aortic smooth muscle cells^{24,36}. Based on the expression pattern and the potential role of *HOX* genes in VW-MSCs we showed that the identified *HOX* code comprising *HOXB7*, *HOXC6* and *HOXC8* helps to discriminate CD44(+)CD90(+)CD73(+)CD105(+)CD34(-)CD45(-) VW-MSCs from mature vascular cells such as mature SMCs and ECs³⁶. This VW-specific *HOX* code was also highly specific for VW-MSCs as compared to undifferentiated pluripotent embryonic stem cells³⁶. This combination of *HOX* genes can also be considered a master regulator to directly convert fibroblasts into VW-MSCs and also used to distinguish them from fibroblasts which otherwise are characterized by a highly similar marker profile. Comparative global profiling of generated VW-MSCs concerning their gene expression and DNA methylation pattern confirmed that ectopic *HOX*-expressing fibroblasts and thus our generated VW-MSCs were closely related to hITA-derived VW-MSC but distinct from control-transduced fibroblasts. However, stromal cell populations derived from various tissues are different, which may result in heterogeneity within the mesenchymal phenotype. Isolated cells from different origins seem to keep expression 'memory' of source specific genes that may travel along during the differentiation process. The cell's signature itself further depends on the quality of the MSC used, which is critically influenced e.g. by the donor age, sex and life style, as well as isolation and cultivation methods³⁷. Recently, a specific gene signature that is shared by a wide-variety of MSC was developed; the so called 'The Rohart MSC test' that accurately distinguished MSC from non-MSC samples³⁷.

With respect to their therapeutic potential, the generated VW-MSCs suppressed lymphocyte proliferation, *in vitro*, and protected mice against radiation-induced pneumopathy. In previous studies we already demonstrated that therapeutically applied VW-MSCs mediate radioprotection

predominately by a paracrine mechanism of action including secretion of the antioxidant enzyme SOD1. This in turn led to the protection of irradiated lung tissue by (i) reducing differentiation of lung-resident (endogenous) stem cells into fibroblasts, and (ii) limiting activation of the usually quiescent lung endothelial cells, which then limited immune cell infiltration (inflammation) and reduced endothelial cell apoptosis⁴⁰⁻⁴². For therapies based on MSCs, safety and efficacy have been proven in the last years. The formation of tumors was almost completely ruled out due to the generally limited differentiation potential of adult stem cells. The directed generation of multipotent stem cells of mesenchymal nature, *in vitro*, is an extremely promising approach for a number of therapeutic applications because single clones harboring vector integrations at safe sites can be selected, expanded and finally differentiated towards the desired MSC-subtype. The possibility and feasibility to obtain patient-specific, vascular wall MSCs from fibroblasts in large amounts by forward programming will potentially open avenues towards novel, MSC-based therapies. Our main hypothesis is that vascular wall-derived MSCs in particular are perfectly suited for the protection and curative treatment of vascular structures, as tissue-specific stem cells mainly support the tissue type from which they originate. In agreement with this notion we reported that VW-MSCs were more potent than bone marrow-derived MSCs to protect lung endothelial cells from the adverse late effects of radiotherapy^{40-42,61}. Thus, the direct *in vitro* conversion of fibroblasts towards VW-MSCs may be an efficient strategy for the treatment of diseases associated with vascular damage and remodeling, e.g. hypertension, ischemic diseases, vascular lesions, or irradiation.

However there are some limitations concerning 'HOX research'. Although HOX gene expression has been genetically manipulated, the identification of distinct HOX target genes in a given cell specification process is still urgently required⁶²⁻⁶⁴. In general, the context within a cell in which certain HOX genes are expressed is important, presumably due to the presence or absence of cofactors and/or coregulators, chromatin accessibility, and epigenetic changes accompanying cell identities⁶⁵. The remaining open question is the precise molecular mechanisms how the VW-MSC specific HOX-code mediates MSC characteristics and what the distinct downstream-targets are.

In summary, we have shown that ectopic expression of *HOXB7*, *HOXC6* and *HOXC8* is sufficient for the successful direct conversion of primary human fibroblasts towards vascular wall-typical MSCs. It remains to be shown whether this triple combination approach resembles the tissue-specific master regulators/transcription factors in VW-MSCs or whether a double combination of HOX candidates or potentially single HOX candidates have the potential to be VW-MSC-specific key transcription factors.

Methods

HOX gene expression vector and transduction

This study was approved by the local ethics committee of the University Hospital Essen. Skin biopsies were taken from healthy control persons after informed consent and cultivated in fibroblast medium⁶⁶. Human fibroblasts were transduced using a lentiviral SIN vector co-expressing the coding sequences of HOXB7, HOXC6 and HOXC8 and the gene encoding Turquoise2 (cyan) fluorescent protein, all separated by 2A esterase elements or control plasmid (same vector without HOX genes)³⁵. 48 hrs after transduction, MSC differentiation was supported by culturing FACS-sorted cyan-positive cells in hMSC-GM media (PromoCell, Heidelberg, Germany). The self-inactivating lentiviral vector for doxycyclin-inducible expression of HOXB7, C6 and C8 (iHOX, Supplementary Fig. S6) was constructed as follows: a plasmid containing the inducible vector backbone, pRRL.PPT.T11-mCherry.PGK.M2.Pre was cut with AgeI, blunted with Klenow fragment of DNA polymerase I and subsequently cut with BsrGI to release the mCherry-CDS fragment. For the HOX co-expression cassette, plasmid pRRL.PPT.SF.HOXB7.2A.C6L.2A.C8.2A.mTurq2.Pre.SIN³⁵ was cut with BamHI, blunted with Klenow fragment and subsequently cut with BsrGI. The coexpression cassette was then isolated and ligated with the vector backbone to generate pRRL.PPT.T11.HOXB7.2A.C6L.2A.mTurq2.PGK.M2.Pre. Transduced cells were treated with doxycycline (0.2-0.5µg/ml) 48hours after transduction. Mock-transduced fibroblasts with or without doxycycline-treatment were used as control.

Trilineage differentiation assay

Differentiation of cultivated MSCs into adipocytes, chondrocytes, and osteocytes was done using ready-to-use differentiation media from Lonza (hMSC Differentiation BulletKit-Adipogenic, PT-3004; -Chondrogenic, PT-3003; -Osteogenic, PT-3002) according to the manufactures instructions. Adipogenic differentiation was verified using Oil red staining, chondrogenic differentiation was verified using collagen type II antibody (Santa Cruz) and immunohistochemistry and osteogenic differentiation was verified using NBT/BCIP staining (Sigma) for alkaline phosphatase activity.

RNA isolation and cDNA synthesis

For RNA isolation, cells were lysed directly in culture dishes as previously described. RNA was isolated using RNeasy Mini Kit (Qiagen, Hilden, Germany) according to the manufacturer's instructions^{36,40}. Real-time RT-PCR analysis was carried out using the desoxoligonucleotide primers listed in Table S3.

Immunohistochemistry and immunofluorescence

Paraffin embedded tissue sections were hydrated using a descending alcohol series, incubated for 10-20 minutes in target retrieval solution (DAKO, Glostrup, Denmark) and incubated with blocking solution (2% FCS/PBS). After permeabilisation, sections were incubated with primary antibodies over night at 4°C. Antigens were detected with anti-rabbit Alexa488 and anti-mouse Alexa555-conjugated secondary antibodies (1/500). Hoechst 33242 iodide was used for nuclei staining. Cells were cultured on gelatine-coated coverslips and were fixed prior staining using 4 % paraformaldehyde for 15 min at room temperature. For staining of nuclear proteins, cells were permeabilized by incubation in 0.1 % (v v) Triton X-100 for 5 min at room temperature. After washing and blocking in PBS with 2 % normal goat serum (serum of secondary antibody host species; Cell Signaling Technology), incubation with the primary antibody for 2-4 hours at room temperature. After washing with PBS, fluorescently labelled secondary antibody was applied for

2 hours. Cells were counterstained with Hoechst 33242 and embedded in fluorescent mounting medium (DAKO). Specimens were imaged on a Zeiss AxioServer fluorescence microscope using the Axiovision acquisition software from Zeiss. Antibodies are listed in Table S4.

Western blot analysis

Whole cell lysates were generated by scraping cells into ice-cold RIPA-P buffer (150 mmol/L NaCl, 1% NP40, 0.5% sodium-desoxycholate, 0.1% sodium-dodecylsulfate, 50 mmol/L Tris/HCL pH 8, 10 mmol/L NaF, 1 mmol/L Na₃VO₄), supplemented with a complete Protease-Inhibitor-Cocktail (Roche) and performing 2-3 freeze-thaw cycles. Protein samples (50–100 µg total protein) were subjected to SDS-PAGE electrophoresis and Western blots were done as previously described using HOXB7, HOXC6, HOXC8, GFP and Nestin (all 1/200) or β-Actin (1/5000) antibodies^{35,36}.

Microarray-based gene expression analysis

Isolation and purification of human vascular wall-resident MSCs (from human thoracic internal artery (hITA) specimens) were excised as previously described^{24,36}. Total RNA was isolated from these cells as well as from control and *HOX*-transduced fibroblasts after flow cytometric sorting for Turquoise2 fluorescence (n=4 for each group). Total RNA integrity was assessed using the 2100 Bioanalyzer (Agilent Technologies, Santa Clara, CA, USA) in combination with the RNA 6000 Nano Kit (Agilent Technologies). Global gene expression profiling was performed using SurePrint G3 Human Gene Expression 8x60k microarrays (AMADID 028005, Agilent Technologies) according to the manufacturer's protocol with an input of 50 ng of total RNA (one-color Low Input Quick Amp Labeling Kit, Agilent Technologies) and as previously described³⁵. Data quality assessment, preprocessing, normalization, and differential expression analyses were conducted using the R Bioconductor packages limma and Agi4x44PreProcess, whereas Benjamini-Hochberg adjusted p-values smaller than 0.5 were considered statistically significant. Unsupervised hierarchical clustering and visualization was performed on gene expression z-scores using the heatmap.2 function from the R package gplots with standard options (Euclidean clustering distance and clustering function "complete"). The accession number for the microarray data reported in this article is ArrayExpress: E-MTAB-6743. GSEA (GenePattern, MsigDB) was used to search for multigene signatures allowing distinguishing classes.

Global DNA methylation analysis

Processing of DNA Methylation arrays was performed on an Illumina (San Diego, CA, USA) platform at the Genome Analysis Center (GAC) of Helmholtz Zentrum München, described as follows. Total gDNA was isolated from primary fibroblasts, control-transduced fibroblasts, generated *HOX*-transduced VW-MSCs and hITA-derived VW-MSCs (n=4 for each group). Bisulfite conversion of 500ng of DNA was done using the EZ DNA Methylation Kit (Zymo Research, Orange, CA, USA) as described recently⁶⁷. Converted gDNA was processed using Infinium®MethylationEPIC BeadChips (Illumina, San Diego, CA, USA) following the Illumina Infinium HD Methylation instructions as described⁶⁷. GenomeStudio (version 2011.1) with Methylation Module (version 1.9.0) was used to process the raw image data generated by the BeadArray Reader. Initial quality control of assay performance was undertaken using "Control Dashboard" provided by GenomeStudio Software, including the assessment of staining, extension, hybridization, target removal, bisulfite conversion, specificity, negative, and non-polymorphic control and checking for number of detected CpG sites.

Cell proliferation/ mixed lymphocyte reaction

Cells were fixed with methanol for 10 min at the indicated time points and subsequently stained with 0.5 % (w/v) crystal violet dye (suspension in methanol: deionized water, 1:5) for 10 min. Excess crystal violet dye was removed by five washes with deionized water on a shaker (10 min for each washing step) and the culture plates dried overnight. Crystal violet was released from cells by incubation with 1% sodium dodecyl sulfate (SDS) for 1-2 hours before optical density measurement at 595 nm. The cell proliferation reagent WST-1 was used as a ready-to-use colorimetric assay for the nonradioactive quantification of cellular viability and cytotoxicity according to the manufacturer's instructions. Optical density measurements were performed 60-90 min after incubation at 450 nm. For mixed lymphocyte reactions, HOX- and control-transduced cells as well as VW-MSCs were plated in 96 well plates (5000 cells per well). After adherence, plates were left untreated or irradiated with 10 Gy. After additional 24 hours, medium was exchanged and lymphocytes of different lines were added (10.000 cells per well): human lymphoma cells [MOLT17 (ACC 36) T cell leukemia, DoHH2 non-Hodgkin's B-cell lymphoma cells (both from Leibniz Institute DSMZ-German Collection of Microorganisms and Cell Cultures, Braunschweig, Germany), Jurkat, Clone E6-1 peripheral blood T lymphocyte, U937 myeloid lineage histiocytic lymphoma (both ATCC/ LGC Standards). After additional 24 hours of co-culture, cell proliferation was determined using the WST-1 colorimetric assay. Values were compared to that one obtained from single lymphocyte cultures.

Whole thorax irradiation (WTI)

Wildtype C57BL/6 mice (mixed gender) received 15 Gy of WTI in a single dose, as previously described⁴⁰. All procedures involving mice were approved by the local institutional Animal Care Committee (Regierungspräsidium Düsseldorf Az84-02.04.2012.A137; 84-02.04.2012.A034). Single cell suspensions of cultured (control and HOX-transduced) fibroblasts (0.2×10^6 cells) were intravenously transplanted into the tail vein of WTI mice 24 hours after irradiation or in sham irradiated (0 Gy) control animals, as previously described^{40,41}. Mice were sacrificed 25-30 weeks post-irradiation and lung tissues collected for further analysis. Total white blood cell counts as well as differential blood cell parameters (lymphocytes, monocytes, and granulocytes) were analyzed in a scil Vet ABC hematology analyzer (scil animal care company, Gurnee, IL) using 10 μ l peripheral blood samples (EDTA anticoagulated) at 3 weeks (within the acute/pneumonitic phase) and 25 weeks (within the chronic/ fibrotic phase) after irradiation

Ex vivo lung tissue culture

Normal human lung tissue samples were obtained during surgery according to local ethical and biohazard regulations and provided from the Department of Thoracic Surgery and Surgical Endoscopy, Ruhrlandklinik, University Hospital Essen. Experiments were approved by the local ethics committee (17-7454-BO; Ethikkommission of the University Medical Faculty, Essen, Germany). Cell cultures of human microvascular endothelial cells (AS-M5) and of human lung tissue specimen were performed as previously described^{41,42}. In brief, fresh lung specimens were dissected and embedded in matrigel using 48-well cluster tissue culture plates, and incubated at 37°C in a humidified atmosphere with 5% CO₂. Embedded pieces as well as cultured endothelial cells were irradiated with 15 Gy using the Isovolt-320-X-ray machine (Seifert-Pantak, East Haven, CT) at 320 kV, 10 mA with a 1.65-mm aluminum filter and further incubated in normal growth media (NGM) alone or NGM supplemented with conditioned media (CM; ratio 1/1), which were derived from cultured fibroblasts, VW-MSCs and Ctrl- and HOX-transduced fibroblasts, for 5 days. Whole cell lysates were generated and analysed by Western blot for the indicated proteins.

Colony-forming unit (CFU) assay

Cells were plated at a density of 100, 250, 500 and 1000 cells per well (triplicates) in 6-well culture dishes. Medium was changed every 2 days. After 10 days' culture, the cells were washed with PBS, fixed with 4% (w/v) paraformaldehyde, and subsequently stained with 0.05% Coomassie Brilliant Blue. Colonies (≥ 50 cells/colony) were counted. The survival curves were established by plotting the log of the surviving fraction ⁴¹.

Statistical analysis

If not otherwise indicated, data were obtained from at least three independent experiments (n=3). Mean values were calculated and used for analysis of standard deviation (SD) or standard error (SEM). Statistical significance was evaluated by 1- or 2-way ANOVA followed by Tukey's or Bonferroni multiple comparisons post-test as indicated. Statistical significance was set at the level of $P \leq 0.05$ (* $P \leq 0.05$, ** $P \leq 0.01$, *** $P \leq 0.005$, ****, # $P \leq 0.001$). Data analysis was performed with Prism 5.0 software (GraphPad, La Jolla, California).

Data availability

The authors declare that all data supporting the findings of this study are available within the article and its supplementary information files or from the corresponding author upon reasonable request. The accession number for the comparative global profiling data reported in this article is ArrayExpress: E-MTAB-6743.

References

- 1 Rashidi, A., DiPersio, J. F., Westervelt, P., Abboud, C. N. & Romee, R. Acute myeloid leukemia presenting with extensive bone marrow necrosis, leukemia cutis and testicular involvement: successful treatment with allogeneic hematopoietic stem cell transplantation. *Bone marrow transplantation* **51**, 454-455, doi:10.1038/bmt.2015.272 (2016).
- 2 Faiella, W. & Atoui, R. Therapeutic use of stem cells for cardiovascular disease. *Clinical and translational medicine* **5**, 34, doi:10.1186/s40169-016-0116-3 (2016).
- 3 Siddiqi, F. & Wolfe, J. H. Stem Cell Therapy for the Central Nervous System in Lysosomal Storage Diseases. *Human gene therapy*, doi:10.1089/hum.2016.088 (2016).
- 4 Sage, E. K., Thakrar, R. M. & Janes, S. M. Genetically modified mesenchymal stromal cells in cancer therapy. *Cytotherapy* **18**, 1435-1445, doi:10.1016/j.jcyt.2016.09.003 (2016).
- 5 Le Blanc, K. *et al.* Mesenchymal stem cells for treatment of steroid-resistant, severe, acute graft-versus-host disease: a phase II study. *Lancet* **371**, 1579-1586, doi:10.1016/S0140-6736(08)60690-X (2008).
- 6 Yu, Y. *et al.* Mesenchymal stem cells with Sirt1 overexpression suppress breast tumor growth via chemokine-dependent natural killer cells recruitment. *Scientific reports* **6**, 35998, doi:10.1038/srep35998 (2016).
- 7 Marofi, F., Vahedi, G., Biglari, A., Esmaeilzadeh, A. & Athari, S. S. Mesenchymal Stromal/Stem Cells: A New Era in the Cell-Based Targeted Gene Therapy of Cancer. *Frontiers in immunology* **8**, 1770, doi:10.3389/fimmu.2017.01770 (2017).
- 8 Conese, M., Carbone, A., Castellani, S. & Di Gioia, S. Paracrine effects and heterogeneity of marrow-derived stem/progenitor cells: relevance for the treatment of respiratory diseases. *Cells, tissues, organs* **197**, 445-473, doi:10.1159/000348831 (2013).
- 9 De Becker, A. & Riet, I. V. Homing and migration of mesenchymal stromal cells: How to improve the efficacy of cell therapy? *World journal of stem cells* **8**, 73-87, doi:10.4252/wjsc.v8.i3.73 (2016).
- 10 Leibacher, J. & Henschler, R. Biodistribution, migration and homing of systemically applied mesenchymal stem/stromal cells. *Stem cell research & therapy* **7**, 7, doi:10.1186/s13287-015-0271-2 (2016).
- 11 Caplan, A. I. & Dennis, J. E. Mesenchymal stem cells as trophic mediators. *Journal of cellular biochemistry* **98**, 1076-1084, doi:10.1002/jcb.20886 (2006).
- 12 Devine, S. M., Cobbs, C., Jennings, M., Bartholomew, A. & Hoffman, R. Mesenchymal stem cells distribute to a wide range of tissues following systemic infusion into nonhuman primates. *Blood* **101**, 2999-3001, doi:10.1182/blood-2002-06-1830 (2003).
- 13 de Witte, S. F. H. *et al.* Immunomodulation By Therapeutic Mesenchymal Stromal Cells (MSC) Is Triggered Through Phagocytosis of MSC By Monocytic Cells. *Stem Cells*, doi:10.1002/stem.2779 (2018).
- 14 Lohan, P., Treacy, O., Griffin, M. D., Ritter, T. & Ryan, A. E. Anti-Donor Immune Responses Elicited by Allogeneic Mesenchymal Stem Cells and Their Extracellular Vesicles: Are We Still Learning? *Frontiers in immunology* **8**, 1626, doi:10.3389/fimmu.2017.01626 (2017).
- 15 Connick, P. & Chandran, S. Mesenchymal stromal cell transplantation modulates neuroinflammatory milieu in amyotrophic lateral sclerosis. *Cytotherapy* **16**, 1031-1032, doi:10.1016/j.jcyt.2014.06.001 (2014).
- 16 Bader, P. *et al.* Effective treatment of steroid and therapy-refractory acute graft-versus-host disease with a novel mesenchymal stromal cell product (MSC-FFM). *Bone marrow transplantation*, doi:10.1038/s41409-018-0102-z (2018).
- 17 Fujii, S. *et al.* Graft-Versus-Host Disease Amelioration by Human Bone Marrow Mesenchymal Stromal/Stem Cell-Derived Extracellular Vesicles Is Associated with Peripheral Preservation of Naive T Cell Populations. *Stem Cells*, doi:10.1002/stem.2759 (2017).
- 18 Le Blanc, K. & Davies, L. C. MSCs-cells with many sides. *Cytotherapy*, doi:10.1016/j.jcyt.2018.01.009 (2018).

- 19 Le Blanc, K. *et al.* Mesenchymal stem cells for treatment of steroid-resistant, severe, acute graft-versus-host disease: a phase II study. *Lancet* **371**, 1579-1586, doi:10.1016/S0140-6736(08)60690-X (2008).
- 20 Jin, H. J. *et al.* Comparative analysis of human mesenchymal stem cells from bone marrow, adipose tissue, and umbilical cord blood as sources of cell therapy. *International journal of molecular sciences* **14**, 17986-18001, doi:10.3390/ijms140917986 (2013).
- 21 Kern, S., Eichler, H., Stoeve, J., Kluter, H. & Bieback, K. Comparative analysis of mesenchymal stem cells from bone marrow, umbilical cord blood, or adipose tissue. *Stem Cells* **24**, 1294-1301, doi:10.1634/stemcells.2005-0342 (2006).
- 22 Zhu, Y. *et al.* Placental mesenchymal stem cells of fetal and maternal origins demonstrate different therapeutic potentials. *Stem cell research & therapy* **5**, 48, doi:10.1186/scrt436 (2014).
- 23 Gotherstrom, C. *et al.* Difference in gene expression between human fetal liver and adult bone marrow mesenchymal stem cells. *Haematologica* **90**, 1017-1026 (2005).
- 24 Klein, D. *et al.* Vascular wall-resident CD44+ multipotent stem cells give rise to pericytes and smooth muscle cells and contribute to new vessel maturation. *PLoS one* **6**, e20540, doi:10.1371/journal.pone.0020540 (2011).
- 25 Jung, Y., Bauer, G. & Nolte, J. A. Concise review: Induced pluripotent stem cell-derived mesenchymal stem cells: progress toward safe clinical products. *Stem Cells* **30**, 42-47, doi:10.1002/stem.727 (2012).
- 26 Kimbrel, E. A. *et al.* Mesenchymal stem cell population derived from human pluripotent stem cells displays potent immunomodulatory and therapeutic properties. *Stem cells and development* **23**, 1611-1624, doi:10.1089/scd.2013.0554 (2014).
- 27 Ma, T., Xie, M., Laurent, T. & Ding, S. Progress in the reprogramming of somatic cells. *Circulation research* **112**, 562-574, doi:10.1161/CIRCRESAHA.111.249235 (2013).
- 28 Okano, H. *et al.* Steps toward safe cell therapy using induced pluripotent stem cells. *Circulation research* **112**, 523-533, doi:10.1161/CIRCRESAHA.111.256149 (2013).
- 29 Klein, D. iPSCs-based generation of vascular cells: reprogramming approaches and applications. *Cellular and molecular life sciences : CMLS*, doi:10.1007/s00018-017-2730-7 (2017).
- 30 Lin, L., Bolund, L. & Luo, Y. Towards Personalized Regenerative Cell Therapy: Mesenchymal Stem Cells Derived from Human Induced Pluripotent Stem Cells. *Current stem cell research & therapy* **11**, 122-130 (2016).
- 31 Sabapathy, V. & Kumar, S. hiPSC-derived iMSCs: NextGen MSCs as an advanced therapeutically active cell resource for regenerative medicine. *Journal of cellular and molecular medicine* **20**, 1571-1588, doi:10.1111/jcmm.12839 (2016).
- 32 Frobel, J. *et al.* Epigenetic rejuvenation of mesenchymal stromal cells derived from induced pluripotent stem cells. *Stem cell reports* **3**, 414-422, doi:10.1016/j.stemcr.2014.07.003 (2014).
- 33 Sheyn, D. *et al.* Human iPSCs Differentiate Into Functional MSCs and Repair Bone Defects. *Stem cells translational medicine*, doi:10.5966/sctm.2015-0311 (2016).
- 34 Steens, J. & Klein, D. Current Strategies to Generate Human Mesenchymal Stem Cells In Vitro. *Stem cells international* **2018**, 6726185, doi:10.1155/2018/6726185 (2018).
- 35 Steens, J. *et al.* In Vitro Generation of Vascular Wall-Resident Multipotent Stem Cells of Mesenchymal Nature from Murine Induced Pluripotent Stem Cells. *Stem cell reports* **8**, 919-932, doi:10.1016/j.stemcr.2017.03.001 (2017).
- 36 Klein, D., Benchellal, M., Kleff, V., Jakob, H. G. & Ergun, S. Hox genes are involved in vascular wall-resident multipotent stem cell differentiation into smooth muscle cells. *Scientific reports* **3**, 2178, doi:10.1038/srep02178 (2013).
- 37 Rohart, F. *et al.* A molecular classification of human mesenchymal stromal cells. *PeerJ* **4**, e1845, doi:10.7717/peerj.1845 (2016).
- 38 Subramanian, A. *et al.* Gene set enrichment analysis: a knowledge-based approach for interpreting genome-wide expression profiles. *Proceedings of the National Academy of Sciences of the United States of America* **102**, 15545-15550, doi:10.1073/pnas.0506580102 (2005).

- 39 Roson-Burgo, B., Sanchez-Guijo, F., Del Canizo, C. & De Las Rivas, J. Insights into the human mesenchymal stromal/stem cell identity through integrative transcriptomic profiling. *BMC genomics* **17**, 944, doi:10.1186/s12864-016-3230-0 (2016).
- 40 Klein, D. *et al.* Therapy with Multipotent Mesenchymal Stromal Cells Protects Lungs from Radiation-Induced Injury and Reduces the Risk of Lung Metastasis. *Antioxidants & redox signaling* **24**, 53-69, doi:10.1089/ars.2014.6183 (2016).
- 41 Klein, D. *et al.* Mesenchymal Stem Cell Therapy Protects Lungs from Radiation-Induced Endothelial Cell Loss by Restoring Superoxide Dismutase 1 Expression. *Antioxidants & redox signaling* **26**, 563-582, doi:10.1089/ars.2016.6748 (2017).
- 42 Wiesemann, A. *et al.* Inhibition of Radiation-Induced Ccl2 Signaling Protects Lungs from Vascular Dysfunction and Endothelial Cell Loss. *Antioxidants & redox signaling*, doi:10.1089/ars.2017.7458 (2018).
- 43 Vierbuchen, T. & Wernig, M. Direct lineage conversions: unnatural but useful? *Nature biotechnology* **29**, 892-907, doi:10.1038/nbt.1946 (2011).
- 44 Pang, Z. P. *et al.* Induction of human neuronal cells by defined transcription factors. *Nature* **476**, 220-223, doi:10.1038/nature10202 (2011).
- 45 Huang, P. *et al.* Direct reprogramming of human fibroblasts to functional and expandable hepatocytes. *Cell stem cell* **14**, 370-384, doi:10.1016/j.stem.2014.01.003 (2014).
- 46 Lai, P. L. *et al.* Efficient Generation of Chemically Induced Mesenchymal Stem Cells from Human Dermal Fibroblasts. *Scientific reports* **7**, 44534, doi:10.1038/srep44534 (2017).
- 47 Yamamoto, K. *et al.* Direct conversion of human fibroblasts into functional osteoblasts by defined factors. *Proceedings of the National Academy of Sciences of the United States of America* **112**, 6152-6157, doi:10.1073/pnas.1420713112 (2015).
- 48 Nam, Y. J. *et al.* Reprogramming of human fibroblasts toward a cardiac fate. *Proceedings of the National Academy of Sciences of the United States of America* **110**, 5588-5593, doi:10.1073/pnas.1301019110 (2013).
- 49 Cherry, A. B. & Daley, G. Q. Reprogramming cellular identity for regenerative medicine. *Cell* **148**, 1110-1122, doi:10.1016/j.cell.2012.02.031 (2012).
- 50 Kurian, L. *et al.* Conversion of human fibroblasts to angioblast-like progenitor cells. *Nature methods* **10**, 77-83, doi:10.1038/nmeth.2255 (2013).
- 51 Klein, D. iPSCs-based generation of vascular cells: reprogramming approaches and applications. *Cellular and molecular life sciences : CMLS* **75**, 1411-1433, doi:10.1007/s00018-017-2730-7 (2018).
- 52 Hou, P. S. *et al.* Direct Conversion of Human Fibroblasts into Neural Progenitors Using Transcription Factors Enriched in Human ESC-Derived Neural Progenitors. *Stem cell reports* **8**, 54-68, doi:10.1016/j.stemcr.2016.11.006 (2017).
- 53 Nakamori, D., Akamine, H., Takayama, K., Sakurai, F. & Mizuguchi, H. Direct conversion of human fibroblasts into hepatocyte-like cells by ATF5, PROX1, FOXA2, FOXA3, and HNF4A transduction. *Scientific reports* **7**, 16675, doi:10.1038/s41598-017-16856-7 (2017).
- 54 Victor, M. B. *et al.* Striatal neurons directly converted from Huntington's disease patient fibroblasts recapitulate age-associated disease phenotypes. *Nature neuroscience*, doi:10.1038/s41593-018-0075-7 (2018).
- 55 Doppler, S. A., Deutsch, M. A., Lange, R. & Krane, M. Direct Reprogramming-The Future of Cardiac Regeneration? *International journal of molecular sciences* **16**, 17368-17393, doi:10.3390/ijms160817368 (2015).
- 56 Dominici, M. *et al.* Minimal criteria for defining multipotent mesenchymal stromal cells. The International Society for Cellular Therapy position statement. *Cytotherapy* **8**, 315-317, doi:10.1080/14653240600855905 (2006).
- 57 Alt, E. *et al.* Fibroblasts share mesenchymal phenotypes with stem cells, but lack their differentiation and colony-forming potential. *Biology of the cell* **103**, 197-208, doi:10.1042/BC20100117 (2011).

- 58 Halfon, S., Abramov, N., Grinblat, B. & Ginis, I. Markers distinguishing mesenchymal stem cells from fibroblasts are downregulated with passaging. *Stem cells and development* **20**, 53-66, doi:10.1089/scd.2010.0040 (2011).
- 59 Lv, F. J., Tuan, R. S., Cheung, K. M. & Leung, V. Y. Concise review: the surface markers and identity of human mesenchymal stem cells. *Stem Cells* **32**, 1408-1419, doi:10.1002/stem.1681 (2014).
- 60 Denu, R. A. *et al.* Fibroblasts and Mesenchymal Stromal/Stem Cells Are Phenotypically Indistinguishable. *Acta haematologica* **136**, 85-97, doi:10.1159/000445096 (2016).
- 61 Klein, D. Vascular Wall-Resident Multipotent Stem Cells of Mesenchymal Nature within the Process of Vascular Remodeling: Cellular Basis, Clinical Relevance, and Implications for Stem Cell Therapy. *Stem cells international* **2016**, 1905846, doi:10.1155/2016/1905846 (2016).
- 62 Bami, M., Episkopou, V., Gavalas, A. & Gouti, M. Directed neural differentiation of mouse embryonic stem cells is a sensitive system for the identification of novel Hox gene effectors. *PLoS one* **6**, e20197, doi:10.1371/journal.pone.0020197 (2011).
- 63 Tkatchenko, A. V. *et al.* Overexpression of Hoxc13 in differentiating keratinocytes results in downregulation of a novel hair keratin gene cluster and alopecia. *Development* **128**, 1547-1558 (2001).
- 64 Ruthala, K. *et al.* Hoxc8 downregulates Mgl1 tumor suppressor gene expression and reduces its concomitant function on cell adhesion. *Molecules and cells* **32**, 273-279, doi:10.1007/s10059-011-0069-8 (2011).
- 65 Gouti, M. & Gavalas, A. Hoxb1 controls cell fate specification and proliferative capacity of neural stem and progenitor cells. *Stem Cells* **26**, 1985-1997, doi:10.1634/stemcells.2008-0182 (2008).
- 66 Stanurova, J. *et al.* Angelman syndrome-derived neurons display late onset of paternal UBE3A silencing. *Scientific reports* **6**, 30792, doi:10.1038/srep30792 (2016).
- 67 Zeilinger, S. *et al.* Tobacco smoking leads to extensive genome-wide changes in DNA methylation. *PLoS one* **8**, e63812, doi:10.1371/journal.pone.0063812 (2013).
- 68 Kaltz, N. *et al.* Novel markers of mesenchymal stem cells defined by genome-wide gene expression analysis of stromal cells from different sources. *Experimental cell research* **316**, 2609-2617, doi:10.1016/j.yexcr.2010.06.002 (2010).
- 69 Sivanathan, K. N., Rojas-Canales, D., Grey, S. T., Gronthos, S. & Coates, P. T. Transcriptome Profiling of IL-17A Preactivated Mesenchymal Stem Cells: A Comparative Study to Unmodified and IFN-gamma Modified Mesenchymal Stem Cells. *Stem cells international* **2017**, 1025820, doi:10.1155/2017/1025820 (2017).
- 70 Kubo, H. *et al.* Identification of mesenchymal stem cell (MSC)-transcription factors by microarray and knockdown analyses, and signature molecule-marked MSC in bone marrow by immunohistochemistry. *Genes to cells : devoted to molecular & cellular mechanisms* **14**, 407-424, doi:10.1111/j.1365-2443.2009.01281.x (2009).

Acknowledgements

We thank Prof. Dr. Verena Jendrossek and Prof. Dr. Peter Horn for hosting our groups and their support of this project. We also thank Mohamed Benchellal and Susanne Skibbe for excellent technical assistance. The work was supported by the Jürgen Manchot Stiftung (Düsseldorf, Germany, JS/DK), the Brigitte und Dr. Konstanze Wegener-Stiftung (Düsseldorf, Germany, DK), and UK Essen/IFORES (D/107-81040, DK).

Author Contributions

JS, AN, KW, HK and DK performed experiments, JH and KU performed microarray and methylation analyses, HJ provided material, HK and DK supervised and analysed results and made the figures; HK and DK designed research and wrote the paper. All authors read and approved the manuscript.

Declaration of Interests

The authors declare no competing interests.

Corresponding author

Correspondence and material requests to Diana Klein

Figure legends

Figure 1

Induction of vascular wall-typical mesenchymal stem cells from adult human fibroblasts

- a** Experimental design for the induction of human MSCs. Primary human fibroblasts were transduced with a lentiviral SIN vector co-expressing the coding sequences of *HOXB7*, *HOXC6* and *HOXC8* and *Turquoise2* (Cyan), which are all co-translationally separated by 2A esterase moieties³⁵. Two to four days after transduction the cells were sorted for cyan fluorescence and cultured in MSC medium. Generated MSCs were characterized 14 days after induction when cells were sufficiently expanded.
- b** Representative scatter plots from the HOX- and control-vector (Ctrl) transduced fibroblasts only expressing *Turquoise2* are shown. The gated cell population (P5) was isolated by FACS.
- c** Representative phase contrast micrographs of cells 10-12 days after flow-cytometric sorting showed typical mesenchymal cell morphology.
- d** Western blot analysis of total HOXB7, HOXC6 and HOXC8 protein expression as well as of Nestin (NES) marker protein expression was performed from whole cell lysates of HOX-transduced and control fibroblasts (FIB) 12-14 days after isolation of transduced cells. Representative blots from two transductions of fibroblasts from two independent donors are shown. Beta-actin (ACTIN) and alpha-tubulin (TUB) were included as loading controls. # indicates fibroblasts derived from different healthy donors.
- e** Sorted HOX-transduced and control fibroblasts were seeded on gelatine-coated cover-slips and HOXB7, HOXC6, HOXC8, and NES expression detected by immunofluorescence using confocal microscopy. Representative photographs are shown.

Figure 2

Characterization of control- and HOX-transduced fibroblasts (generated VW-MSCs)

- a** Relative amounts of transcripts of the indicated genes were determined by qRT-PCR in HOX- and control vector-transduced fibroblasts 12-14 days after transduction and flow-cytometry based cell isolation (biological replicates: n=4-6 per group and gene; *P* by two-way ANOVA, followed by post-hoc Tukey's multiple comparisons test: *****P* ≤ 0.001). For the detection of endogenous *HOX* gene expression, desoxy-oligonucleotide-primer pairs located in the 3'UTR as well as in the 5'UTR were used, which are not present in the retroviral expression vector containing only the CDS. For overall detection of retroviral vector expression, the woodchuck hepatitis virus posttranscriptional regulatory element (wPRE) was used.
- b** Verification of induced conversion into MSCs. FACS-purified HOX-transduced and control fibroblasts were differentiated into adipocytes, osteocytes and chondrocytes, *in vitro*. Differentiation was observed within 14 days after induction of differentiation (DM) as shown by Oil red staining, by histochemical staining for alkaline phosphatase (ALP), or by immunocytochemistry for collagen type II expression. Representative photographs are shown (biological replicates: n=3-4). Magnification 400x (Scale bars: 25 μm). As control, respective cells were cultured in normal growth media (NGM).
- c** Trilineage differentiation along the mesodermal lineage was further quantified after 14 days of culture within differentiation media by qRT-PCR analysis of peroxisome proliferator-activated

receptor gamma (PPAR γ), alkaline phosphatase (ALP), osteocalcin (ON) and aggrecan (ACAN) expression levels. Data were presented as mean \pm SEM (biological replicates: n=7 for each group and gene).

d HOX-transduced and control fibroblasts were grafted together with human endothelial cells (AS-M5) in Matrigel subcutaneously into NMRI nude mice for 14 days. Immunofluorescent analysis of re-isolated plug tissues was performed by confocal microscopy. Immunoreactivity to human CD31 is shown in red, expression of the reporter fluorescence protein Turquoise2 in green. Arrows point to the regular assembly of cyan-positive vascular wall MSCs that tightly surround the vessels formed by human endothelial cells. Representative images of n=4 independent experiments are shown. DAPI was used for nuclei staining. Scale bars: 50 μ m.

e CFU Assay. Control and HOX-transduced and FACS-sorted fibroblasts were plated at low densities (100-1000 cells/ well) in plastic culture dishes and subsequently cultured for 10 days. Coomassie Brilliant Blue stained colonies were counted and the surviving fraction (colony formation) was calculated. *P* by two-tailed t-test: ***P* \leq 0.01 (biological replicates: n=8-10 for each group).

Figure 3

Global gene expression and DNA methylation analysis

a Global transcriptome heatmaps (top 100 variant genes; left) of VW-MSCs and HOX- as well as control-transduced fibroblasts as determined by microarray analysis and selected MSC marker genes ('The Rohart MSC test'; right) (biological replicates: n=4 per group).

b Principle component analysis indicates that generated (HOX-transduced) VW-MSCs exhibit global gene expression profiles similar to those of hITA-derived VW-MSCs.

c Hierarchical clustering of the beta-values (top 100 variants) of the global DNAm profiles of primary fibroblasts (FIB), control-transduced fibroblasts, generated HOX-transduced VW-MSCs (HOX) and hITA-derived VW-MSCs (biological replicates: n=4 per group).

d Principle component analysis using the Rohart MSC signature genes extracted from the global DNAm profiles ³⁷.

Figure 4

Gene Expression Profiling of generated fibroblast-derived VW-MSCs

a GSEA was performed using gene sets specific for different MSCs. Genes highly expressed in human MSC derived from placental tissue (PL-MSC) as compared to human skin fibroblasts were used ³⁹.

b Membrane associated genes (top panel) and a CD selection (bottom panel) highly expressed in bone marrow-derived MSC (BM-MSC) as compared with stromal cells derived from umbilical veins (UVSC) were used ⁶⁸.

c Genes highly expressed in untreated BM-MSC as compared to (pre-activated) IFN- γ treated BM-MSC (top panel) ⁶⁹, as well as genes expressed selectively in BM-MSC compared with fibroblasts, osteoblasts, chondrocytes and adipocytes ⁷⁰.

d Genes highly expressed in VW-MSC compared to VW-MSCs upon HOX silencing were used³⁶. Top panel represents all significantly altered genes upon HOX gene silencing; bottom panel represents genes highly expressed in VW MSC as compared to those downregulated in VW-MSCs upon HOX silencing.

e Genes highly expressed in VW-MSC as compared to human aortic smooth muscle cells (hAoSMC) were used (unpublished data set). cDNA microarray analysis using AffymetrixH DNA chips was performed in order to identify potential VW-MSC markers as compared to the mature vascular wall cells. Resulting significantly different expressed genes were grouped according to gene ontology and genes involved in the immune response (54 genes in total of which 34 genes were highly upregulated in VW-MSCs) as well as involved in angiogenesis (56 genes in total of which 22 genes were highly upregulated in VW-MSCs) were used as gene sets. Genes were drawn according to their rank from left (high expression in Ctrl) to right (high expression in VW-MSC derived from HOX-transduced fibroblasts) and gene sets plotted on top with each black bar representing a gene. The enrichment score is plotted in on the vertical axis. Specific gene sets were listed in the Supplementary Table S2.

Figure 5

Therapeutic potential of generated fibroblast-derived VW-MSCs

a Verification of lymphocyte proliferation inhibition: HOX-transduced and control fibroblasts were co-cultured with different lymphoma cells (DoHH2, Jurkat, MOLT17, and U937) for 24 hours. VW-MSCs were used as positive control. Cell-cycle arrested, irradiated (10Gy, 24 hours prior to co-culture) fibroblasts/MSCs were used to exclude possible effects mediated by their proliferation. (bottom diagram). Cell proliferation was determined using a WST-1 reagent-based tetrazolium reduction assay and related to proliferation of lymphoma (LYM) cells alone (biological replicates: n=5-6 per group and lymphoma cell line; *P* by two-way ANOVA followed by post-hoc Tukey's multiple comparisons test: **P* ≤ 0.05; ***P* ≤ 0.01; ****P* ≤ 0.005; #*P* ≤ 0.001).

b Therapeutically applied generated VW-MSCs limit radiation-induced lung fibrosis and endothelial cell loss: C57BL/6 mice were left untreated or received a 15Gy whole thorax irradiation (WTI). Single cell suspensions of cultured cells (0.2×10^6 cells) were intravenously transplanted via tail vein injection into WTI mice 24 hours after irradiation. 25 weeks later, sections of paraffin-embedded lung tissue was performed and connective tissue stained by Masson's Goldner Trichrome. Sham irradiated (0Gy) animals served as control. Representative light microscopy images from two different experiments (#1, #2) are shown (scale bar = 100µm).

c Quantification of lung fibrosis was done by determining the Ashcroft scores blinded to the genotype and treatment conditions. Data are presented as means ± SEM. ***P* ≤ 0.01; *****P* ≤ 0.001 by one-way ANOVA followed by post-hoc Tukey's test (n=15-25 mice per group).

d Endothelial VE-Cadherin (VE-CAD) and TGFβ expression was analyzed in whole protein lysates from mice lungs using Western blot analysis 25 weeks post irradiation (n=5-6 per group). Beta-actin was included as loading control. Representative blots from lungs of three different mice per group were shown.

e Cultured normal lung tissue fragments embedded in growth factor reduced matrigel were exposed to irradiation with 15 Gy, subsequently cultured in normal growth media (NGM) alone or NGM supplemented with conditioned media (CM; ratio 1/1), which were derived from cultured fibroblasts, VW-MSCs and Ctrl- and HOX-transduced fibroblasts (generated VW-MSCs). Expression levels of the indicated proteins were analyzed in whole protein lysates using Western

blot analysis at 5 days after radiation and subsequent CM treatment. Representative blots from four different experiments are shown (n=4).

f Cultured AS-M5 endothelial cells were exposed to irradiation with 15 Gy, subsequently cultured in normal growth media (NGM) or NGM supplemented with CM. Expression levels of the indicated proteins were analyzed in whole protein lysates using Western blot analysis at 96 hours after radiation and subsequent growth factor treatment. Representative blots from four different experiments are shown (n=3).

Figures

Figure 1

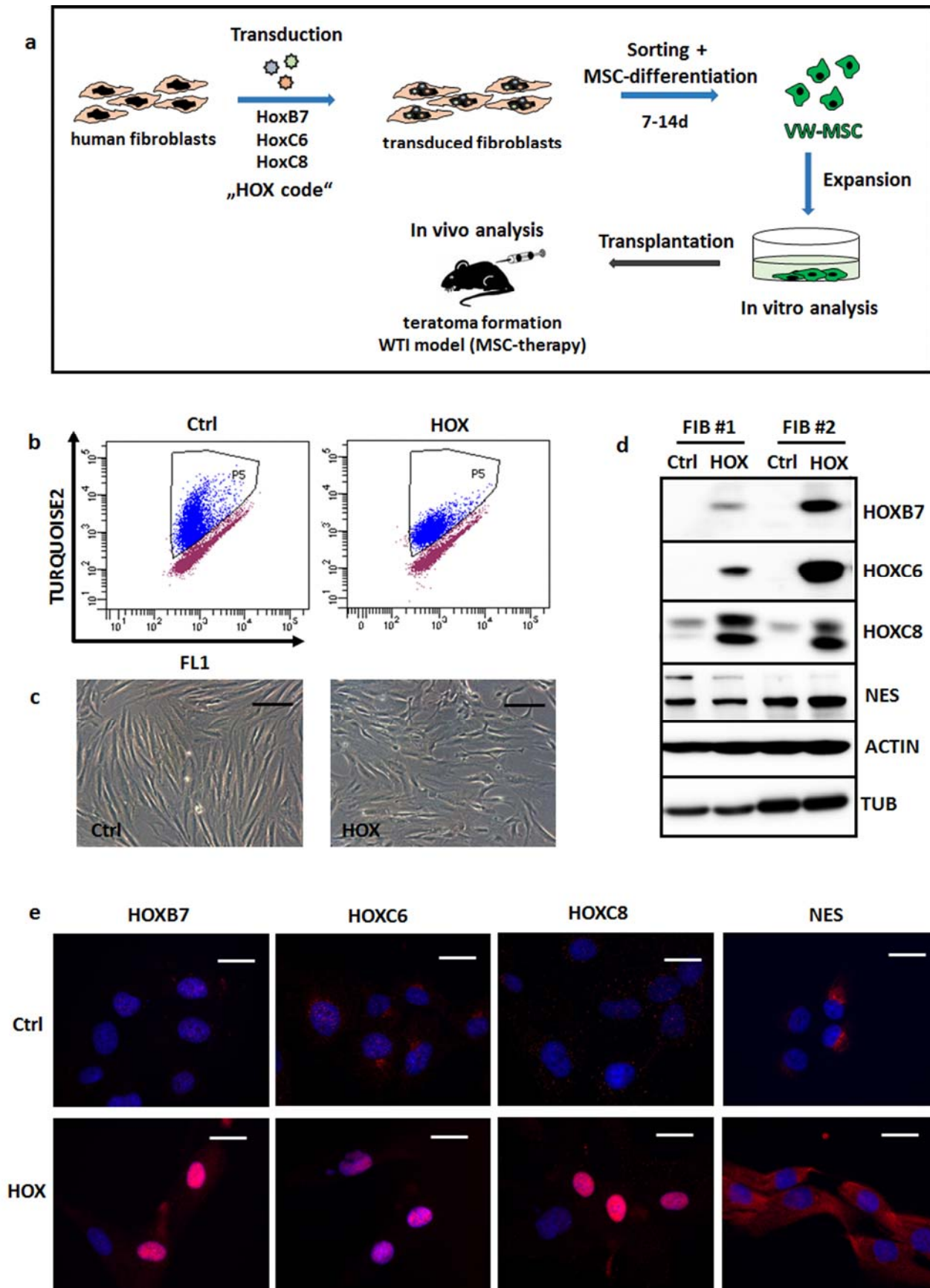


Figure 2

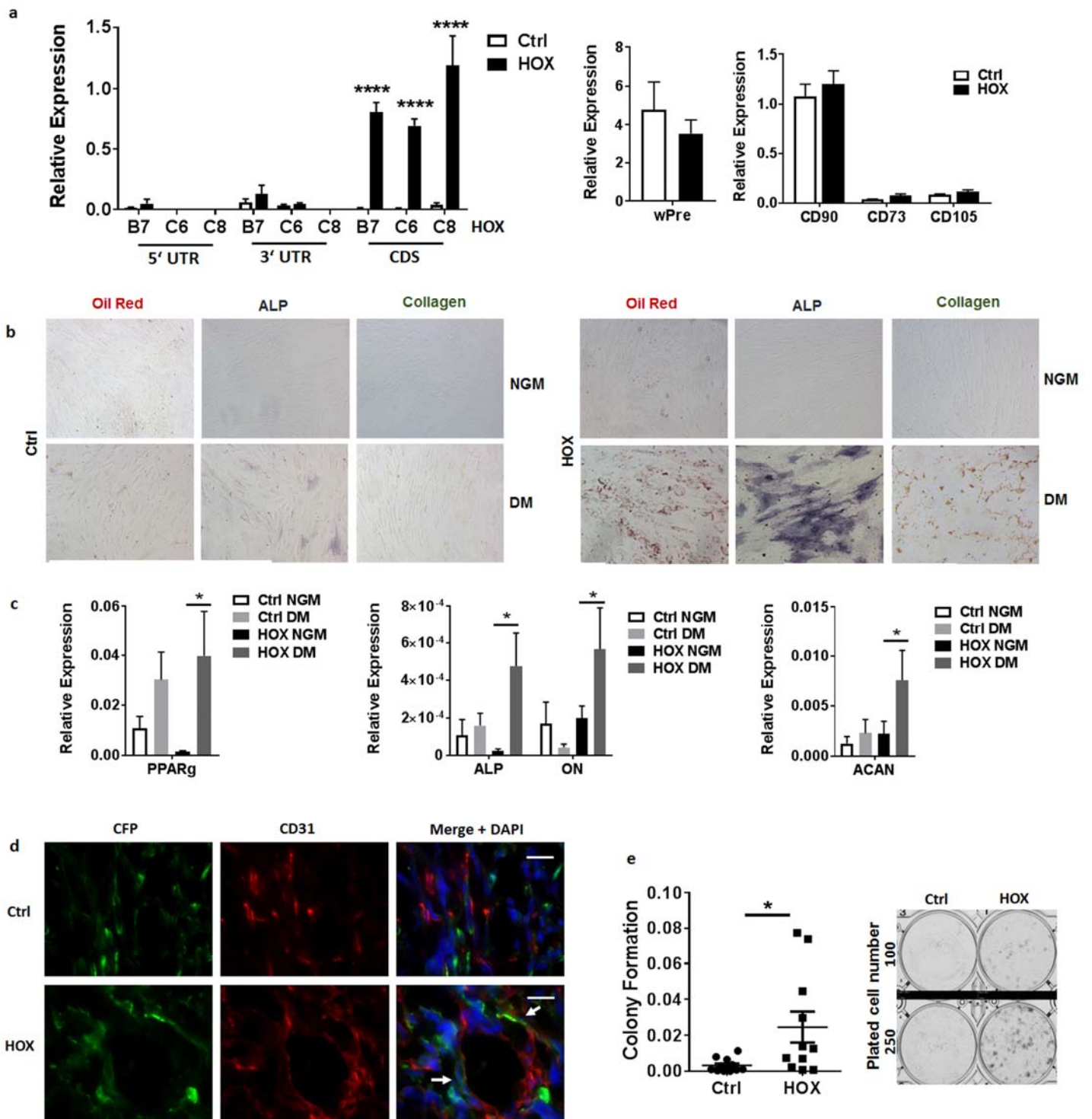


Figure 3

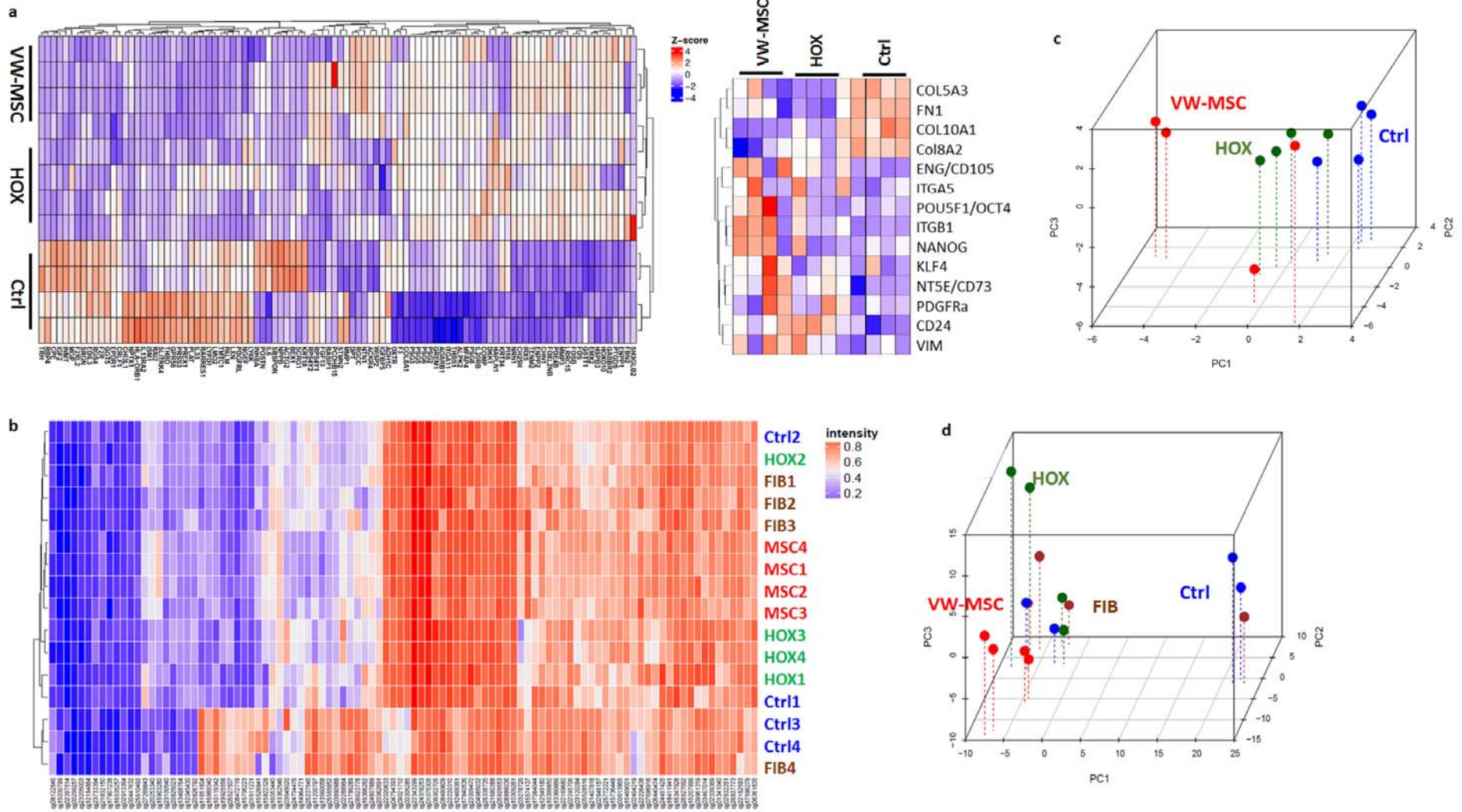


Figure 4

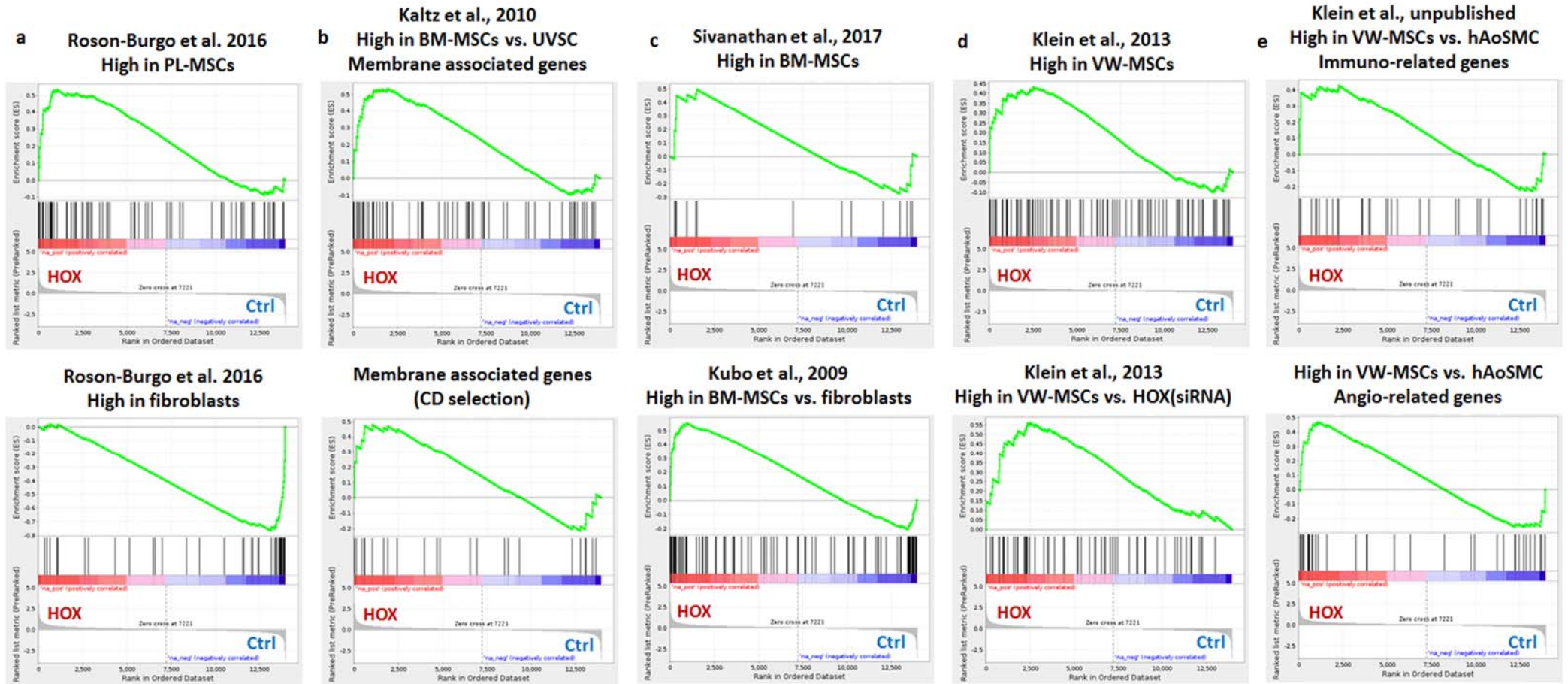


Figure 5

